

Coupling Coefficients of Different Disk Microresonators with Whispering Gallery Modes

Trubin A. A.

National Technical University of Ukraine “Igor Sikorsky Kyiv Polytechnic Institute”, Ukraine

E-mail: atrubin@ukrpost.net

The coupling coefficients of the disk microresonators, consisting of different dielectrics, are presented. The analytical expressions for the coupling coefficients are obtained. The basic regularities of the coupling coefficient changing on the structure parameter variations are considered. The coupling coefficients as functions of main structure parameters are studied. The calculation results of the transmission coefficients as well as the reflection coefficients of the bandpass filters, building up on different disk microresonators with different modes are presented. The S-matrix frequency dependences of the bandpass filters on different disk microresonators in the infrared wavelength range are calculated. The dielectric Q-factor values, necessary for acceptable measure of the scattering are determined. The amplitude-frequency characteristics of the bandpass filters on the vertically coupled as well as laterally coupled disc microresonators are investigated. Most optimal configurations of coupled microresonators, allowing to achieve the best scattering characteristics are determined. It's showed that using of microresonators with whispering gallery modes allow relatively easy obtain frequency-symmetrical characteristics of the filters.

Key words: microresonator; coupling coefficient; whispering gallery mode; S-matrix; filter

Introduction

Disk dielectric microresonators with whispering gallery (WG) modes inscribes in the planar integral circuits quite naturally. Today, ones are being actively studied for purpose of their application in the different devices of the optical, infrared and terahertz wavelength ranges [1–7]. Eigenoscillations of two disk dielectric microresonators were considered in [4–7], but its coupling coefficients were not calculated and not studied in full measure. For calculation and optimization of the device parameters, it's convenient to carry out on basis of electrodynamic modeling with using coupling coefficients [8].

The goal of the present work is the analytical calculation of the coupling coefficients of different disk microresonators with WG modes in the open space. In this article, we also use the scattering theory for S-matrix coefficients calculation of different microresonator bandpass filters.

1 Eigenoscillation field calculation of the disk microresonator

For the coupling coefficients calculation, information about microresonator eigenoscillation fields is necessary. Most simple analytical presentation the field within dielectric cylinder can be obtained in the form of so-called one-wave approximation [9]. Toward this

end, an electromagnetic field is written in the cylindrical coordinate system (ρ, α, z) (see fig. 1a), located in the microresonator center, approximately in the form of hybrid standing wave of the circular dielectric waveguide section:

$$e_\rho = \left[e_1 \frac{\beta_z}{\beta} J'_m(\beta\rho) + h_1 m \frac{i\omega\mu_0}{\beta} \cdot \frac{J_m(\beta\rho)}{\beta\rho} \right] \cdot \begin{Bmatrix} \sin m\alpha \\ \cos m\alpha \end{Bmatrix} \cdot \begin{Bmatrix} \cos \beta_z z \\ -\sin \beta_z z \end{Bmatrix}$$

$$e_\alpha = \left[e_1 m \frac{\beta_z}{\beta} \cdot \frac{J_m(\beta\rho)}{\beta\rho} + h_1 \frac{i\omega\mu_0}{\beta} \cdot J'_m(\beta\rho) \right] \cdot \begin{Bmatrix} \cos m\alpha \\ -\sin m\alpha \end{Bmatrix} \cdot \begin{Bmatrix} \cos \beta_z z \\ -\sin \beta_z z \end{Bmatrix}$$

$$e_z = e_1 J_m(\beta\rho) \begin{Bmatrix} \sin m\alpha \\ \cos m\alpha \end{Bmatrix} \begin{Bmatrix} \sin \beta_z z \\ \cos \beta_z z \end{Bmatrix} \quad (1)$$

$$h_\rho = \left[e_1 m \frac{i\omega\varepsilon_1}{\beta} \cdot \frac{J_m(\beta\rho)}{\beta\rho} - h_1 \frac{\beta_z}{\beta} \cdot J'_m(\beta\rho) \right] \cdot \begin{Bmatrix} \cos m\alpha \\ -\sin m\alpha \end{Bmatrix} \cdot \begin{Bmatrix} \sin \beta_z z \\ \cos \beta_z z \end{Bmatrix}$$

$$h_\alpha = \left[-e_1 \frac{i\omega\varepsilon_1}{\beta} \cdot J'_m(\beta\rho) + h_1 m \frac{\beta_z}{\beta} \cdot \frac{J_m(\beta\rho)}{\beta\rho} \right] \cdot \begin{Bmatrix} \sin m\alpha \\ \cos m\alpha \end{Bmatrix} \cdot \begin{Bmatrix} \sin \beta_z z \\ \cos \beta_z z \end{Bmatrix}$$

$$h_z = h_1 J_m(\beta\rho) \begin{Bmatrix} \cos m\alpha \\ -\sin m\alpha \end{Bmatrix} \begin{Bmatrix} \cos \beta_z z \\ -\sin \beta_z z \end{Bmatrix}$$

Here e_1, h_1 — is the electrical and magnetic field amplitudes; β, β_z — is the wave numbers; r_0 — is the radius; L — is the height of the disk microresonator; $J'_m(x)$ — is the derivative of Bessel function of the first kind of the m -th order [10].

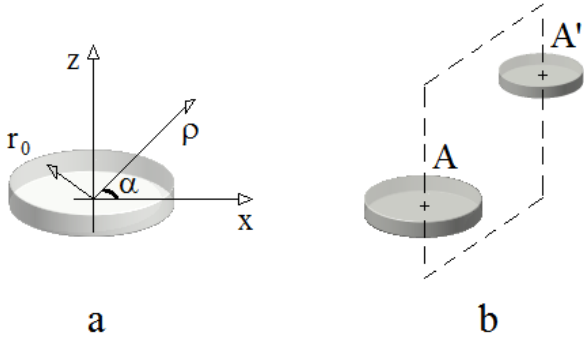


Fig. 1. A — cylindrical coordinate system in the center of the disk microresonator; b — symmetry plane (AA') of two different disk microresonators.

The constant values $e_1, h_1; \beta, \beta_z$ approximate expression can be determined from the simple equations: $e_1 = ae_0; h_1 = ah_0$ and

$$\begin{aligned} h_0 + e_0 &= \frac{J_{m-1}(p_\perp)}{p_\perp J_m(p_\perp)} + \frac{Y_{m-1}(p_{0\perp})}{p_{0\perp} Y_m(p_{0\perp})} \\ h_0 - e_0 &= \frac{J_{m+1}(p_\perp)}{p_\perp J_m(p_\perp)} + \frac{Y_{m+1}(p_{0\perp})}{p_{0\perp} Y_m(p_{0\perp})} \end{aligned} \quad (2)$$

The dimensionless parameters: $p_\perp = \beta r_0; p_{0\perp} = \beta_0 r_0$, and also $p_z = \beta_z L/2; p_{0z} = \beta_{0z} L/2$ can be calculated from combined equations:

$$\begin{aligned} &\left[\frac{\varepsilon_{1r}}{\beta} \frac{J'_m(\beta r_0)}{J_m(\beta r_0)} + \frac{1}{\beta_0} \frac{Y'_m(\beta_0 r_0)}{Y_m(\beta_0 r_0)} \right] \cdot \\ &\cdot \left[\frac{1}{\beta} \frac{J'_m(\beta r_0)}{J_m(\beta r_0)} + \frac{1}{\beta_0} \frac{Y'_m(\beta_0 r_0)}{Y_m(\beta_0 r_0)} \right] = \\ &= \left(\frac{m\beta_z}{k_0 r_0} \right)^2 \left(\frac{1}{\beta^2} + \frac{1}{\beta_0^2} \right)^2 \end{aligned} \quad (3)$$

$\beta^2 + \beta_z^2 = k_1^2; -\beta_0^2 + \beta_z^2 = k_0^2; \beta^2 - \beta_{0z}^2 = k_0^2;$
as well as, for the HE_{nml}^\pm and EH_{nml}^\mp modes:

$$\begin{aligned} \beta_{0z} &= \beta_z \cdot \begin{Bmatrix} -\text{ctg } \beta_z L/2 \\ \text{tg } \beta_z L/2 \end{Bmatrix} \\ \varepsilon_{1r} \beta_{0z} &= \beta_z \cdot \begin{Bmatrix} \text{tg } \beta_z L/2 \\ -\text{ctg } \beta_z L/2 \end{Bmatrix} \end{aligned} \quad (4)$$

$Y'_m(x)$ — is the derivative of Bessel function of the second kind of the m -th order.

The n defines the number of half-waves, located in the radial direction inside dielectric cylinder, the defines half-waves number, located in the direction of z -axis in the microresonator material; the is integer. Sign $+(-)$ in the cases of HE_{nml}^\pm mode corresponds to an even (odd) mode distribution of z -component of the magnetic field; and the $-(+)$ for the EH_{nml}^\mp mode corresponds to an even (odd) mode distribution of z -component of the electric field in the microresonator (see fig.1) relative to the plane of symmetry $z = 0$ (fig. 1a).

Equations (3) and (4) must be solved simultaneously.

2 Calculation of coupling coefficient

The fields and frequencies of several microresonator coupled oscillations defines by values of the coupling coefficients. In the common case, the coupling coefficient can be determined as a surface integral:

$$\kappa_{sn} = \frac{i}{2\omega_0 w_n (1 + \delta_{sn})} \oint_{s_n} \left\{ \left[\vec{e}_s, \vec{h}_n^* \right] + \left[\vec{e}_n^*, \vec{h}_s \right] \right\} \vec{n} ds, \quad (5)$$

expressed via the eigenmode field (\vec{e}_s, \vec{h}_s) of one (s -th) microresonator on the surface of another (n -th) microresonator. Here $s, n = 1, 2$; and \vec{n} — is the normal to the surface s_n of n -th microresonator, ω_0 — is the resonance frequency; w_n — is the energy, stored in the dielectric of n -th microresonator.

As follow from [8], eigenoscillations of two identical microresonators take on form of even- and odd- modes spatial field distributions with respect to symmetry plane, located between ones (fig. 1b). In this case (5): $\kappa_{11} = \kappa_{22} = i\tilde{k}; \kappa_{12} = \kappa_{21} = \kappa$ and $b_2^1 = +b_1^1; b_2^2 = -b_1^2; \lambda_{1,2} = i\tilde{k} \pm \kappa$, are corresponding to the cophased, or even, and antiphased, or odd, field distribution of the coupling oscillations.

The real and imaginary parts of the coupling coefficient can take positive values as well as negative ones. As follow from (5), the coupling coefficients of two different microresonators are not equal to one another: $\kappa_{12} \neq \kappa_{21}$.

The integral (5) can be calculated, based on early known analytical expression for the coupling coefficients, of the Cylindrical DRs in the Rectangular metal waveguide. In this case, required analytical expressions for mutual coupling coefficients κ_{12} , can be received by transferring the waveguide walls to the infinity. Using necessary expressions, after simplifications, we obtain:

2.1 Case A.

In the case of two different microresonators, with the same parity of each field on α and on the indexes m_s

($s = 1, 2$), relative to the plane of symmetry: $y_s - y = 0$ ($s = 1, 2$) (see fig. 2a), the mutual coupling coefficients can be obtained in the form: in the area: $\Delta z \geq r_1 + r_2$ (fig. 2a):

$$\begin{aligned} \kappa_{1,2} = & i\kappa_0^{12} \cdot \int_0^\infty \left\{ e^{-i(m_1 - m_2)\pi/2} \cos[(m_1 - m_2)\Delta\alpha] \cdot \right. \\ & \cdot H_{m_1 - m_2}^{(2)}(k_0\Delta\rho\sqrt{1 - \xi^2}) \mp (-1)^{m_1 m_2} e^{-i(m_1 + m_2)\pi/2} \cdot \\ & \cdot \cos[(m_1 + m_2)\Delta\alpha] H_{m_1 + m_2}^{(2)}(k_0\Delta\rho\sqrt{1 - \xi^2}) \left. \right\} \cdot \\ & \cdot [F_{11}(\xi)F_{12}(\xi)^* + F_{21}(\xi)F_{22}(\xi)^*] \cdot \cos(k_0\Delta x\xi) d\xi \quad (6) \end{aligned}$$

where the top sign of (6) corresponds to even-mode field distribution, relative to the plane of symmetry and the bottom one corresponds to odd-mode field distribution (see 1); $\sin \Delta\alpha = \Delta z / \Delta\rho$; $\Delta\rho = \sqrt{\Delta y^2 + \Delta z^2}$; $\Delta x = x_2 - x_1$; $\Delta y = y_2 - y_1$; $\Delta z = |z_2 - z_1|$;

$$\kappa_0^{12} = \frac{32}{\varepsilon_{2r} w(2)} \cdot \frac{p_{2z}}{q_{2z}} \cdot \frac{q_{1\perp}}{q_{2\perp}}$$

Here $p_{sz} = \beta_{sz} L_s / 2$; $q_{s\perp} = k_0 r_s$; $q_{sz} = k_0 L_s / 2$; r_s — is the radius; L_s — is the height; ε_{sr} — relative dielectric permittivity of the s -th disk microresonator ($s = 1, 2$);

$$\begin{aligned} F_{1s}(\xi) = & \frac{e_{0s}}{\beta_{zs}} \left\{ \left[k_s^2 \sqrt{1 - \xi^2} J'_{m_s}(p_{s\perp}) J_{m_s}(q_{s\perp} \sqrt{1 - \xi^2}) - k_0 \beta_s J_{m_s}(p_{s\perp}) J'_{m_s}(q_{s\perp} \sqrt{1 - \xi^2}) \right] \cdot \right. \\ & \cdot \frac{1}{\beta_{sz}^2 - (k_0 \xi)^2} \cdot \left[\frac{\beta_{sz} \cos p_{sz} \sin q_{sz} \xi - k_0 \xi \sin p_{sz} \cos q_{sz} \xi}{\beta_{sz} \sin p_{sz} \cos q_{sz} \xi - k_0 \xi \cos p_{sz} \sin q_{sz} \xi} \right] + \\ & + \left[\beta_s J_{m_s}(p_{s\perp}) J'_{m_s}(q_{s\perp} \sqrt{1 - \xi^2}) - k_0 \sqrt{1 - \xi^2} J'_{m_s}(p_{s\perp}) J_{m_s}(q_{s\perp} \sqrt{1 - \xi^2}) \right] \cdot \\ & \cdot \frac{1}{\beta_s^2 - k_0^2 (1 - \xi^2)} \left[\frac{k_s^2 \xi \sin p_{sz} \cos q_{sz} \xi - k_0 \beta_{sz} \cos p_{sz} \sin q_{sz} \xi}{k_s^2 \xi \cos p_{sz} \sin q_{sz} \xi - k_0 \beta_{sz} \sin p_{sz} \cos q_{sz} \xi} \right] \left. \right\} - \\ & - h_{0s} m_s \frac{\xi (k_s^2 - k_0^2)}{p_{s\perp} k_0 \sqrt{1 - \xi^2}} J_{m_s}(p_{\perp}) J_{m_s}(q_{s\perp} \sqrt{1 - \xi^2}) \cdot \\ & \cdot \frac{1}{\beta_{sz}^2 - (k_0 \xi)^2} \left[\frac{\beta_{sz} \sin p_{sz} \cos q_{sz} \xi - k_0 \xi \cos p_{sz} \sin q_{sz} \xi}{\beta_{sz} \cos p_{sz} \sin q_{sz} \xi - k_0 \xi \sin p_{sz} \cos q_{sz} \xi} \right] \quad (7) \end{aligned}$$

$$\begin{aligned} F_{2s}(\xi) = & (k_s^2 - k_0^2) \left\{ e_{0s} m_s \frac{1}{p_{s\perp} k_0^2 \sqrt{1 - \xi^2}} J_{m_s}(p_{s\perp}) J_{m_s}(q_{s\perp} \sqrt{1 - \xi^2}) - h_{0s} \frac{1}{\beta_s^2 - k_0^2 (1 - \xi^2)} \cdot \right. \\ & \cdot \left. \left[\beta_s J_{m_s}(p_{s\perp}) J'_{m_s}(q_{s\perp} \sqrt{1 - \xi^2}) - k_0 \sqrt{1 - \xi^2} J'_{m_s}(p_{s\perp}) J_{m_s}(q_{s\perp} \sqrt{1 - \xi^2}) \right] \right\} \cdot \\ & \cdot \frac{1}{\beta_{sz}^2 - (k_0 \xi)^2} \left[\frac{\beta_{sz} \sin p_{sz} \cos q_{sz} \xi - k_0 \xi \cos p_{sz} \sin q_{sz} \xi}{\beta_{sz} \cos p_{sz} \sin q_{sz} \xi - k_0 \xi \sin p_{sz} \cos q_{sz} \xi} \right] \end{aligned}$$

e_0 ; h_0 — are the normalized amplitudes, defined from (2);

$$\begin{aligned} w(s) = & \left[(e_{s0} - h_{s0})^2 [J_{m_s-1}^2(p_{s\perp}) - J_{m_s}(p_{s\perp}) J_{m_s-2}(p_{s\perp})] + \right. \\ & + (e_{s0} + h_{s0})^2 [J_{m_s+1}^2(p_{s\perp}) - J_{m_s}(p_{s\perp}) J_{m_s+2}(p_{s\perp})] + \\ & + 2 \left(\frac{\beta_s}{k_s} h_{s0} \right)^2 [J_{m_s}^2(p_{s\perp}) - J_{m_s-1}(p_{s\perp}) J_{m_s+1}(p_{s\perp})] \left. \right] \left[\begin{array}{l} 2p_{sz} + \sin 2p_{sz} \\ 2p_{sz} - \sin 2p_{sz} \end{array} \right] + \\ & + \left[\left(\frac{k_s}{\beta_{sz}} e_{s0} - \frac{\beta_{sz}}{k_s} h_{s0} \right)^2 [J_{m_s-1}^2(p_{s\perp}) - J_{m_s}(p_{s\perp}) J_{m_s-2}(p_{s\perp})] + \right. \\ & + \left(\frac{k_s}{\beta_{sz}} e_{s0} + \frac{\beta_{sz}}{k_s} h_{s0} \right)^2 [J_{m_s+1}^2(p_{s\perp}) - J_{m_s}(p_{s\perp}) J_{m_s+2}(p_{s\perp})] + \\ & + 2 \left(\frac{\beta_s}{\beta_{sz}} e_{s0} \right)^2 [J_{m_s}^2(p_{s\perp}) - J_{m_s-1}(p_{s\perp}) J_{m_s+1}(p_{s\perp})] \left. \right] \left[\begin{array}{l} 2p_{sz} - \sin 2p_{sz} \\ 2p_{sz} + \sin 2p_{sz} \end{array} \right] \quad (8) \end{aligned}$$

$k_s = \sqrt{\varepsilon_{sr}} k_0$; $k_0 = \omega_0 / c$; ω_0 — is the circular resonance frequency; c — is the light velocity.

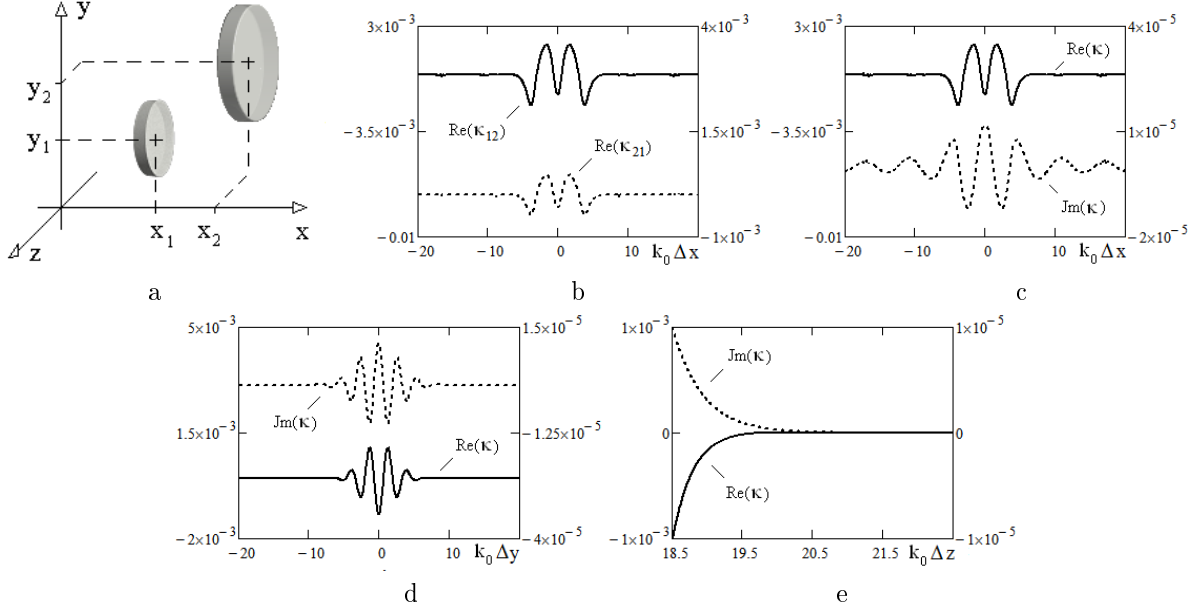


Fig. 2. Rectangular coordinate system and two laterally coupled different disk microresonators in the open space (a). Mutual coupling coefficients as function coordinates of the microresonators with $\varepsilon_{1r} = 16$; $\varepsilon_{2r} = 9, 6$; $\Delta_1 = \Delta_2 = 0, 2$; for $HE_{1,m,1}^+$ modes; ($m_1 = 20$; $m_2 = 24$): $k_0\Delta y = 0$; $k_0\Delta z = q_{1\perp} + q_{2\perp}$ (b, c); $k_0\Delta x = 0$; $k_0\Delta z = q_{1\perp} + q_{2\perp}$ (d, e).

2.2 Case B.

In the case of different disk microresonators with equal parity of the field distribution (see fig. 3a) relative to symmetry plane AA' (fig. 1b):

in the area: $\Delta z > L_1/2 + L_2/2$ obtains

$$\begin{aligned} \kappa_z^{1,2} = & i\kappa_0^{12} \cdot \int_0^\infty \frac{e^{-i\sqrt{1-\kappa^2}k_0\Delta z}}{\sqrt{1-\kappa^2}} \cdot \left\{ (k_1^2 - k_0^2)(k_2^2 - k_0^2) \cdot \right. \\ & \cdot C_1(\kappa)C_2(\kappa)^* \left[\cos(m_1 - m_2)\Delta\psi J_{m_1-m_2}(k_0\Delta\rho\kappa) \pm (-1)^{m_1m_2} \cos(m_1 + m_2)\Delta\psi J_{m_1+m_2}(k_0\Delta\rho\kappa) \right] + \\ & \left. + D_1(\kappa)D_2(\kappa)^* \left[\cos(m_1 - m_2)\Delta\psi J_{m_1-m_2}(k_0\Delta\rho\kappa) \mp (-1)^{m_1m_2} \cos(m_1 + m_2)\Delta\psi J_{m_1+m_2}(k_0\Delta\rho\kappa) \right] \right\} \kappa d\kappa \quad (9) \end{aligned}$$

where $\sin \Delta\psi = \Delta y/\Delta\rho$; $\Delta\rho = \sqrt{\Delta x^2 + \Delta y^2}$;

$$\begin{aligned} C_s(\kappa) = & \left\{ e_{s0}m_s \frac{1}{p_{s\perp}k_0\kappa} J_{m_s}(p_{s\perp})J_{m_s}(q_{s\perp}\kappa) - h_{s0} \frac{1}{r_s(\beta_s^2 - k_0^2\kappa^2)} \cdot \right. \\ & \cdot \left. [p_{s\perp}J_{m_s}(p_{s\perp})J'_{m_s}(q_{s\perp}\kappa) - q_{s\perp}\kappa J_{m_s}'(p_{s\perp})J_{m_s}(q_{s\perp}\kappa)] \right\} \cdot \\ & \cdot \frac{1}{\beta_{sz}^2 - k_0^2(1-\kappa^2)} \left[\frac{\beta_{sz} \sin p_{sz} \cos q_{sz} \sqrt{1-\kappa^2} - k_0 \sqrt{1-\kappa^2} \cos p_{sz} \sin q_{sz} \sqrt{1-\kappa^2}}{\beta_{sz} \cos p_{sz} \sin q_{sz} \sqrt{1-\kappa^2} - k_0 \sqrt{1-\kappa^2} \sin p_{sz} \cos q_{sz} \sqrt{1-\kappa^2}} \right] \quad (10) \end{aligned}$$

$$\begin{aligned} D_s(\kappa) = & \frac{e_{s0}}{\beta_{sz}q_{s\perp}} \left\{ [k_0^2 p_{s\perp} J_{m_s}(p_{s\perp}) J'_{m_s}(q_{s\perp}\kappa) - k_s^2 q_{s\perp} \kappa J_{m_s}'(p_{s\perp}) J_{m_s}(q_{s\perp}\kappa)] \cdot \right. \\ & \cdot \frac{1}{\beta_{sz}^2 - k_0^2(1-\kappa^2)} \left[\frac{k_0 \sqrt{1-\kappa^2} \sin p_{sz} \cos q_{sz} \sqrt{1-\kappa^2} - \beta_{sz} \cos p_{sz} \sin q_{sz} \sqrt{1-\kappa^2}}{\beta_{sz} \sin p_{sz} \cos q_{sz} \sqrt{1-\kappa^2} - k_0 \sqrt{1-\kappa^2} \cos p_{sz} \sin q_{sz} \sqrt{1-\kappa^2}} \right] - \\ & \left. - \frac{1}{\beta_s^2 - (k_0\kappa)^2} [p_{s\perp} J_{m_s}(p_{s\perp}) J'_{m_s}(q_{s\perp}\kappa) - q_{s\perp} \kappa J_{m_s}'(p_{s\perp}) J_{m_s}(q_{s\perp}\kappa)] \cdot \right. \end{aligned}$$

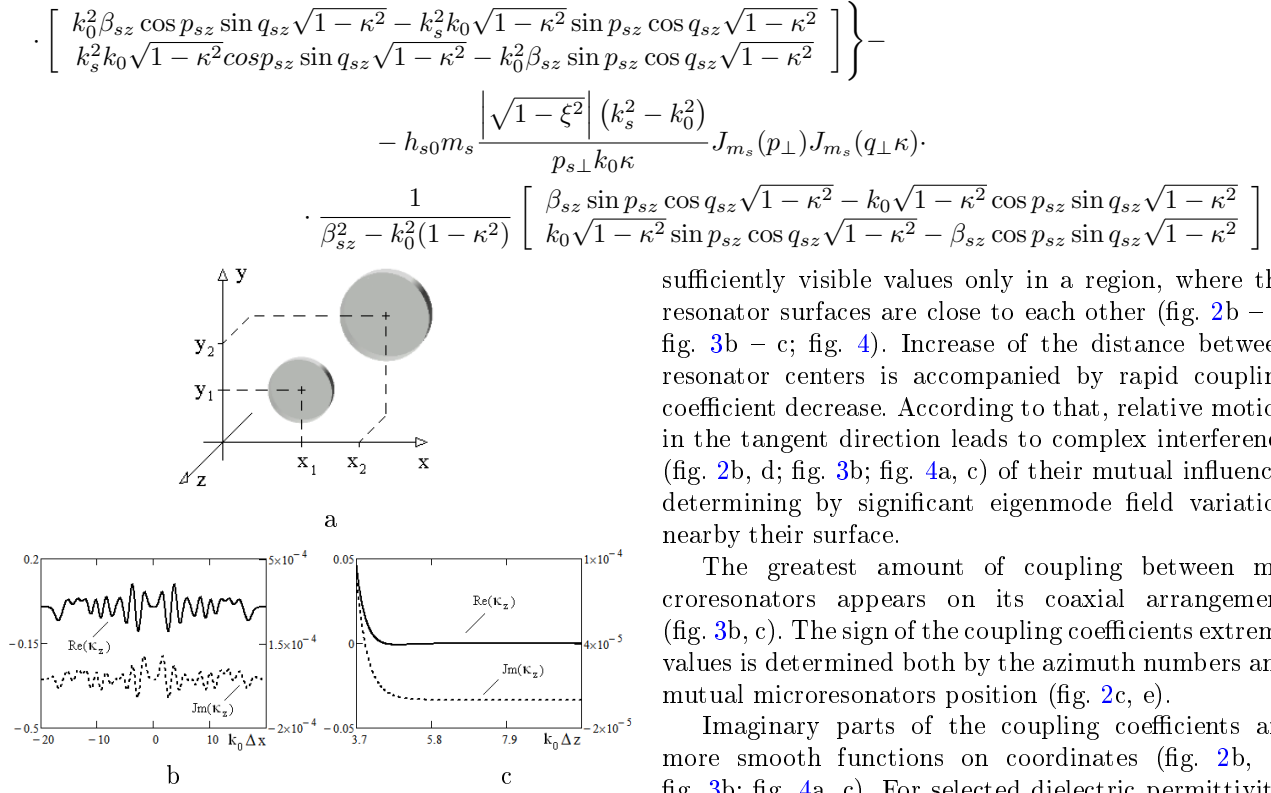


Рис. 3. Vertically coupled different disk microresonators (a). Coupling coefficient dependencies for the $HE_{1,m,1}^+$ modes; ($m_1 = 20$; $m_2 = 24$): $\varepsilon_{1r} = 16$; $\varepsilon_{2r} = 9.6$; $\Delta_1 = \Delta_2 = 0, 2$; $k_0 \Delta y = 0$; $k_0 \Delta z = 3, 7$ (b); $k_0 \Delta x = 0$; $k_0 \Delta y = 1, 8$ (c).

The integral convergence provides by choice of the radical signs for $\xi > 1$: $\sqrt{\xi^2 - 1} = -i\sqrt{1 - \xi^2}$ in the (9), (10), as well as for $\sqrt{\kappa^2 - 1} = -i\sqrt{1 - \kappa^2}$ in the (6), (7).

The coupling between disk microresonator and the open space following from Helmholtz-Kirchhoff's integral theorem can be obtained as:

$$\kappa_s = \frac{32i}{\varepsilon_{sr} \omega(s)} \cdot \frac{p_{sz}}{q_{sz}} \cdot \int_0^1 \left\{ (k_s^2 - k_0^2)^2 \left| C_s(\sqrt{1 - \kappa^2}) \right|^2 + \left| D_s(\sqrt{1 - \kappa^2}) \right|^2 \right\} d\kappa \quad (11)$$

3 Coupling coefficient analysis

Discovered relationships valid for any eigenoscillations of the disk microresonators in the open space, but a greatest interest presents the WG modes, as it's well known, possessed a highest possible quality.

Fig. 2, 3, 4 are showing coupling coefficient dependences on Disk microresonator centers, composed of the dielectric with the relative permittivity $\varepsilon_{1r} = 16$; $\varepsilon_{2r} = 9,6$ and the comparative dimensions $\Delta_s = L_s/2r_s = 0, 2$. Right ordinate axes on fig. 2c - e; fig. 3, 4 shows imaginary part of the coupling coefficients. It's clear, that the real part of the coupling coefficients has

sufficiently visible values only in a region, where the resonator surfaces are close to each other (fig. 2b - e; fig. 3b - c; fig. 4). Increase of the distance between resonator centers is accompanied by rapid coupling coefficient decrease. According to that, relative motion in the tangent direction leads to complex interference (fig. 2b, d; fig. 3b; fig. 4a, c) of their mutual influence, determining by significant eigenmode field variation nearby their surface.

The greatest amount of coupling between microresonators appears on its coaxial arrangement (fig. 3b, c). The sign of the coupling coefficients extreme values is determined both by the azimuth numbers and mutual microresonators position (fig. 2c, e).

Imaginary parts of the coupling coefficients are more smooth functions on coordinates (fig. 2b, d; fig. 3b; fig. 4a, c). For selected dielectric permittivity, its values are approximately one tenth degrees to the real parts.

The fig. 2b is showing difference between two resonator coupling coefficients.

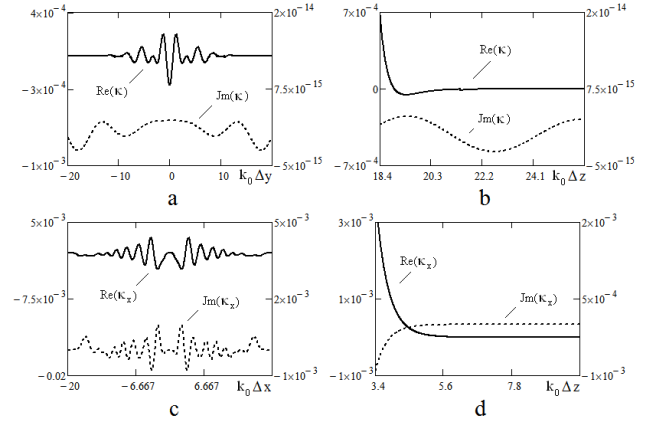


Рис. 4. Coupling coefficients as functions of the coordinates for different disk microresonators in the position showed in fig. 2a (a, b) $k_0 \Delta x = 0$; $k_0 \Delta z = 1, 05(q_{1\perp} + q_{2\perp})$ (a); $k_0 \Delta x = k_0 \Delta y = 0$ (b); in the position showed in fig. 3a (c, d); $k_0 \Delta y = 0$; $k_0 \Delta z = q_{1\perp} + q_{2\perp}$ (c); $k_0 \Delta x = 0$; $k_0 \Delta z = 3.7$ (d); $\varepsilon_{1r} = 16$; $\varepsilon_{2r} = 9, 6$; $\Delta_1 = \Delta_2 = 0, 2$, for the $EH_{1,m,1}^+$ modes.

4 Filter parameters calculation

Obtained results allow us to create electrodynamic models of various filters in the millimeter, terahertz or infrared wavelength ranges. As can be seen the coupling between not adjacent microresonators in the filters will

be very small in comparison with coupling between adjacent ones, that allows simply to build filters with symmetrically parameters of the scattering. Different microresonator using in this case will allow to obtain much clean stop-bands.

The transmission T and the reflection coefficient of different DR system for the bandpass filter configuration in the transmission line can be obtained by using perturbation theory:

$$T = T_0 - \frac{1}{B(\omega)} \sum_{s=1}^N B_s^+(\omega); R = R_0 - \frac{1}{B(\omega)} \sum_{s=1}^N B_s^-(\omega) \quad (12)$$

where T_0 , R_0 are the transmission and reflection coefficients of the transmission line without DRs;

$$B_s^\pm(\omega) = \det \begin{bmatrix} b_1^1 Q_{11}(\omega) & \dots & Q_1^D b_{N,1}^s \tilde{k}_{N1}^{\pm+} & \dots & b_1^N Q_{N1}(\omega) \\ b_2^1 Q_{12}(\omega) & \dots & 0 & \dots & b_2^N Q_{N2}(\omega) \\ \vdots & \dots & \vdots & \dots & \vdots \\ b_N^1 Q_{1N}(\omega) & \dots & 0 & \dots & b_N^N Q_{NN}(\omega) \end{bmatrix} \quad (13)$$

$$B(\omega) =$$

$$\det \begin{bmatrix} b_1^1 Q_{11}(\omega) & b_1^2 Q_{21}(\omega) & \dots & b_1^N Q_{N1}(\omega) \\ b_2^1 Q_{12}(\omega) & b_2^2 Q_{22}(\omega) & \dots & b_2^N Q_{N2}(\omega) \\ \vdots & \vdots & \dots & \vdots \\ b_N^1 Q_{1N}(\omega) & b_N^2 Q_{2N}(\omega) & \dots & b_N^N Q_{NN}(\omega) \end{bmatrix}$$

For simplicity we proposed that $\tilde{k}_{N1}^{++} = \tilde{k}_{11}^{-+} = k_L$; where k_L — is the coupling coefficient of the 1-th and the N -th microresonator with the transmission input (output) line of the filter.

Here for different microresonators, the functions $Q_{st}(\omega)$ are dependent on the partial DR and the coupled oscillation numbers:

$$Q_{st}(\omega) = 2i \frac{\omega - \tilde{\omega}^s}{\omega_0} Q_t^D + \frac{\omega}{\omega_0}; \quad (14)$$

$Q_t^D = \omega_0 w_t / P_t^D$; $P_t^D = \omega_0 \frac{\epsilon''_t}{2} \int_{V_t} |\vec{e}_t|^2 dv$ — is the loss power in the dielectric of t -th DR; b_t^s — is the complex amplitude of t -th resonator of the s -th mode $\tilde{\omega}^s$ frequency of the filter [8].

The fig. 5 and 6 show results of the calculation of bandpass filter S -parameters matrix, that is built up on different disk microresonators with $HE_{1,m,1}^+$ mode. It's proposed, that coupling coefficients of the terminal resonators k_L with transmission lines are known. Mutual coupling coefficients where obtained from (6 - 11).

It's seen, that in consequence of rapidly coupling coefficients decrease, all S -parameters are symmetrical

functions on the frequency. As we used a large number of resonators, the S_{21} squareness was obtained well.

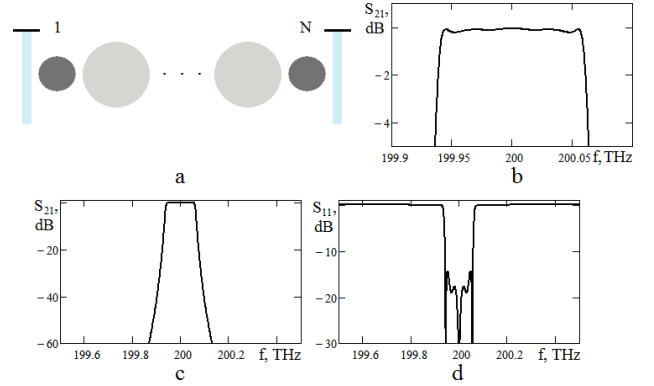


Рис. 5. Sketch of bandpass filter on laterally coupled different disk microresonators (a). S -matrix responses of the 7-section bandpass filter on $HE_{1,m,1}^+$ mode as functions of the frequency (b - e). The coupling coefficients of the terminal resonators with transmission lines: $k_L = 7 \cdot 10^{-4}$; the 1-th and the N -th microresonator parameters are $\epsilon_{1r} = 16$; $Q_1^D = 10^6$; $m_1 = 20$; another resonator parameters are $\epsilon_{2r} = 9, 6$; $Q_2^D = 2 \cdot 10^6$; $m_2 = 24$.

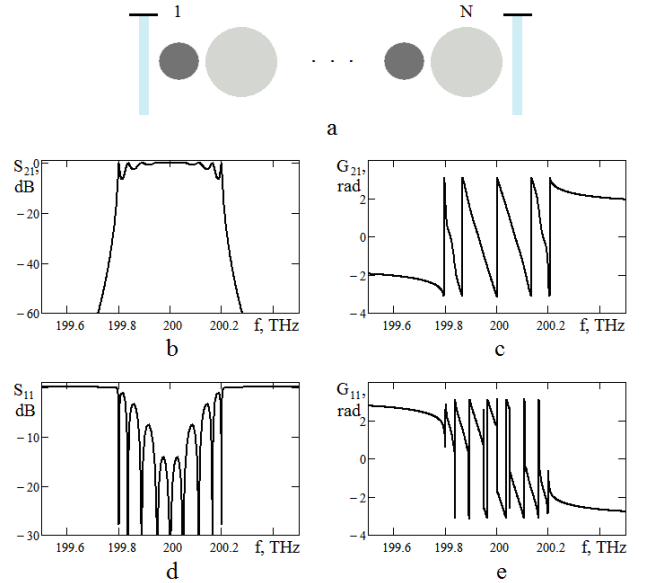


Рис. 6. Bandpass filter on repeating different disk microresonators (a). S -matrix responses of the 9-section bandpass filter with $HE_{1,m,1}^+$ mode as functions of the frequency (b - e). The coupling coefficients of the terminal resonators with transmission lines: $k_L = 9, 0 \cdot 10^{-4}$; the odd microresonator parameters are $\epsilon_{1r} = 16$; $Q_1^D = 10^6$; the even microresonator parameters are $\epsilon_{2r} = 9, 6$; $Q_2^D = 2 \cdot 10^6$.

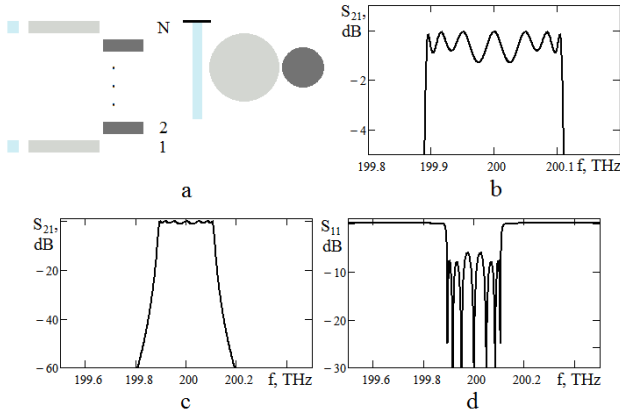


Рис. 7. Bandpass filter on vertically coupled disk microresonators (a). S -matrix responses of the 7-section bandpass filter with $HE_{1,m,1}^+$ mode as functions of the frequency (b - e). The coupling coefficients of the terminal resonators with transmission lines: $k_L = 5 \cdot 10^{-4}$; microresonator parameters are $\varepsilon_{1r} = 9, 6$; $Q_1^D = 2 \cdot 10^6$; $\varepsilon_{2r} = 16$; $Q_2^D = 10^6$

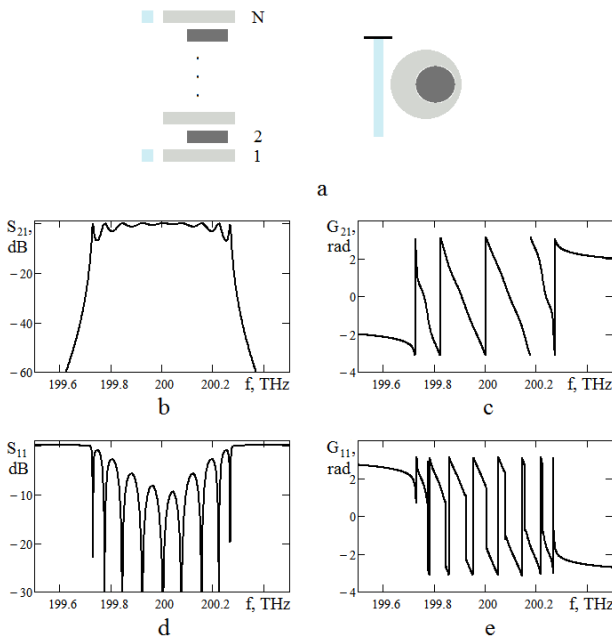


Рис. 8. Bandpass filter on repeating vertically coupled different disk microresonators (a). S -matrix responses of the 9-section bandpass filter with $HE_{1,m,1}^+$ mode as functions of the frequency (b - e). The coupling coefficients of the terminal resonators with transmission lines: $\varepsilon_{1r} = 9, 6$; odd microresonator parameters are $\varepsilon_{1r} = 9, 6$; $Q_1^D = 10^6$; even microresonator parameters are $\varepsilon_{2r} = 16$, $Q_2^D = 10 \cdot 10^6$.

Conclusions

Analytical relationships for the coupling coefficients of the different disk microresonators in the Open space have been obtained and investigated.

It's stated, that the coupling between not adjacent microresonators in the filters is small in comparison with coupling between adjacent ones that allows simply building bandpass filters with symmetrically scattering parameters.

The filters on WG modes microresonators has acceptable frequency responses and after optimization maybe recommended for utilization on multiplexing of various communication systems.

References

- [1] Popović M. A., Manolatu C. and Watts M. R. (2016) Coupling-induced resonance frequency shifts in coupled dielectric multi-cavity filters. *Optics express*, Vol. 14, No. 3, pp. 1208-1222. DOI: 10.1364/OE.14.001208
- [2] Benson T.M., Boriskina S.V., Sewell P., Vukovic A., Greedy S.C. and Nosich A.I. (2006) Micro-Optical Resonators for Microlasers and Integrated Optoelectronics. In: *Janz S., Ctyroky J., Tanev S. (eds) Frontiers in Planar Lightwave Circuit Technology. NATO Science Series II: Mathematics, Physics and Chemistry*, Vol 216. Springer, Dordrecht. DOI: 10.1007/1-4020-4167-5_02
- [3] Khalil H., Bila S., Aubourg M., Baillargeat D., Verdeyme S., Puech J., Lapierre L., Delage C. and Chartier T. (2009) Topology Optimization of Microwave Filters Including Dielectric Resonators. *Microwave Conference, 2009. EuMC 2009. European*, pp. 687-690.
- [4] Smotrova E. I., Nosich A. I., Benson T. M. and Sewell P. (2006) Optical Coupling of Whispering-Gallery Modes of Two Identical Microdisks and Its Effect on Photonic Molecule Lasing. *IEEE Journal of Selected Topics in Quantum Electronics*, Vol. 12, Iss. 1, pp. 78-85. DOI: 10.1109/JSTQE.2005.862940
- [5] Boriskina S.V. (2007) Coupling of whispering-gallery modes in size mismatched microdisk photonic molecules. *Optics Letters*, Vol 32, No. 11, pp. 1557-1559. DOI: 10.1364/OL.32.001557
- [6] Jun-Jie Li, Jia-Xian Wang and Yong-Zhen Huang (2007) Mode coupling between first- and second-order whispering-gallery modes in coupled microdisks. *Optics Letters*, Vol. 32, No. 11. pp. 1563-1565. DOI: 10.1364/OL.32.001563
- [7] Preu S., Schwefel H. G. L., Malzer S., Dohler G. H., Wang L. J., Hanson M., Zimmerman J. D. and Gossard A. C. (2008) Coupled whispering gallery mode resonators in the Terahertz frequency range. *Optics Express*, Vol. 16, No. 10, pp. 7336-7343. DOI: 10.1364/OE.16.007336
- [8] Trubin A. A. (2016) *Lattices of Dielectric Resonators*, Vol 53, Springer International Publishing, 159 p. DOI : 10.1007/978-3-319-25148-6
- [9] Trubin, A. A. (2015) Coupling coefficients of the disk dielectric microresonators with whispering gallery modes. *Visn. NTUU KPI, Ser. Radiotekh. radioaparotobuduv.*, no. 61, pp. 60-71.
- [10] Abramowitz M. and Stegun I. (1964) *Handbook of mathematical functions with Formulas, Graphs and Mathematical Tables Applied Mathematics Series No. 55*. National bureau of standards.

Коефіцієнти зв'язку різних дискових мікрорезонаторів з коливаннями шепочучої галереї

Трубін О. О.

Приведено результати розрахунків коефіцієнтів взаємного зв'язку різноманітних дискових мікрорезонаторів з коливаннями шепочучої галереї, виконаних із різних матеріалів. Отримані аналітичні вирази для коефіцієнтів зв'язку. Розглянуті основні закономірності зміни зв'язку при варіації параметрів структури. Приведені результати розрахунків коефіцієнтів передачі та відбиття смугових фільтрів, побудованих на різних мікрорезонаторах з різними видами коливань. Розраховані частотні залежності матриці розсіювання смугових фільтрів на різних дискових мікрорезонаторах інфрачервоного діапазону довжин хвиль. Визначені значення добротності діелектрику, необхідні для отримання прийнятних характеристик розсіювання. Досліджені амплітудно-частотні характеристики смугових фільтрів на вертикально зв'язаних, а також зв'язаних по боковій стінці дискових мікрорезонаторах. Встановлено найбільш оптимальні конфігурації зв'язаних мікрорезонаторів, які дозволяють досягати найкращих характеристик розсіювання. Показано, що застосування мікрорезонаторів з коливаннями шепочучої галереї дозволяє відносно просто отримувати частотно-симетричні характеристики розсіювання фільтрів.

Ключові слова: мікрорезонатор; коефіцієнт зв'язку; режим шепочучої галереї; S-матриця; фільтр

Коэффициенты связи различных дисковых микрорезонаторов с колебаниями шепчущей галереи

Трубин А. А.

Приведены результаты расчета коэффициентов взаимной связи различных дисковых микрорезонаторов с колебаниями шепчущей галереи, выполненных из разных материалов. Получены аналитические выражения для коэффициентов связи. Рассмотрены основные закономерности изменения связи при вариации параметров структуры. Приведены результаты расчета коэффициентов передачи и отражения полосовых фильтров, построенных на различных микрорезонаторах с разными видами колебаний. Рассчитаны частотные зависимости матрицы рассеяния полосовых фильтров на различных дисковых микрорезонаторах инфракрасного диапазона длин волн. Определены значения добротности диэлектрика, необходимые для получения приемлемых характеристик рассеяния. Исследованы амплитудно-частотные характеристики полосовых фильтров на вертикально связанных, а также связанных по боковой стенке дисковых микрорезонаторах. Установлены наиболее оптимальные конфигурации связанных микрорезонаторов, позволяющие достигать наилучших характеристик рассеяния. Показано, что применение микрорезонаторов с колебаниями шепчущей галереи позволяет относительно просто получать частотно-симметричные характеристики рассеяния фильтров.

Ключевые слова: микрорезонатор ; коэффициент связи ; режим шепчущей галереи ; S-матрица ; фильтр